

ChemComm

Chemical Communications

Accepted Manuscript

This article can be cited before page numbers have been issued, to do this please use: N. Roamcharern, P. Punnabhum, H. Graham, F. P. Seib and Z. Rattray, *Chem. Commun.*, 2026, DOI: 10.1039/D6CC02515C.



This is an Accepted Manuscript, which has been through the Royal Society of Chemistry peer review process and has been accepted for publication.

Accepted Manuscripts are published online shortly after acceptance, before technical editing, formatting and proof reading. Using this free service, authors can make their results available to the community, in citable form, before we publish the edited article. We will replace this Accepted Manuscript with the edited and formatted Advance Article as soon as it is available.

You can find more information about Accepted Manuscripts in the [Information for Authors](#).

Please note that technical editing may introduce minor changes to the text and/or graphics, which may alter content. The journal's standard [Terms & Conditions](#) and the [Ethical guidelines](#) still apply. In no event shall the Royal Society of Chemistry be held responsible for any errors or omissions in this Accepted Manuscript or any consequences arising from the use of any information it contains.

COMMUNICATION

Ensemble and single particle analysis of doxorubicin silk nanoparticles

Napaporn Roamcharern^a, Panida Punnabhum^a, Harriet Graham^a, F. Philipp Seib^{a,b,c}, Zahra Rattray^{a*}Received 00th January 20xx,
Accepted 00th January 20xx

DOI: 10.1039/x0xx00000x

Adsorption-loaded silk nanoparticles exploit protein electrostatics and β -sheet-rich architecture to achieve high doxorubicin loading and pH-responsive release, while preserving silk structure. Ensemble and single-particle analyses reveal exceptional formulation uniformity, while *in vitro* studies confirm preserved cytotoxicity against MDA-MB-231 human breast cancer cells.

Doxorubicin is a widely used chemotherapeutic agent, yet its clinical utility is limited by cumulative cardiotoxicity and chemoresistance, prompting the development of nanocarriers that have partially mitigated some of these limitations.¹⁻⁴ Formulation complexity, heterogenous drug loading, and adverse effects of these formulations, continue to constrain translational performance of doxorubicin nanoparticles.⁵ Silk fibroin nanoparticles, distinguished by their β -sheet-rich structure and tuneable surface chemistry, offer favourable physicochemical characteristics,⁶⁻⁸ including controlled release,^{9, 10} enhanced internalization and lysosomotropic delivery,¹¹ and improved solubility.^{9, 12} Despite growing interest in silk nanoparticles as nanoscale delivery vehicles, the impact of drug loading strategies exploiting these features to govern drug release behaviour remains underexplored.¹³⁻¹⁶ Here, we investigate adsorption-based loading of doxorubicin onto pre-formed silk nanoparticles as a chemically defined strategy to spatially confine doxorubicin without disrupting β -sheet-rich protein architecture. We hypothesised that adsorption would preserve silk secondary structure while directly linking protein electrostatics to pH-responsive release behaviour.

Silk nanoparticles prepared by semi-batch antisolvent precipitation formed monodisperse, spherical assemblies with negative surface charge, consistent with β -sheet-rich structure. Adsorption of doxorubicin resulted in high encapsulation efficiency (~90%) without measurable changes in particle size or morphology (Fig. 1a-e, Fig. S2, Fig. S3, and Fig. S4). A modest

shift in surface charge toward less negative values was observed, consistent with electrostatic interactions between protonated amines on doxorubicin and anionic silk residues, while retaining colloidal stability. Fourier-transform infrared spectroscopy (FTIR) analysis confirmed retention of β -sheet-dominated secondary structure of the nanoparticles following doxorubicin adsorption. The preservation of silk-like features indicates that doxorubicin remains localised at or near the nanoparticle surface rather than penetrating the β -sheet-rich core (Fig. 1f, g and Fig. S5).^{17, 18}

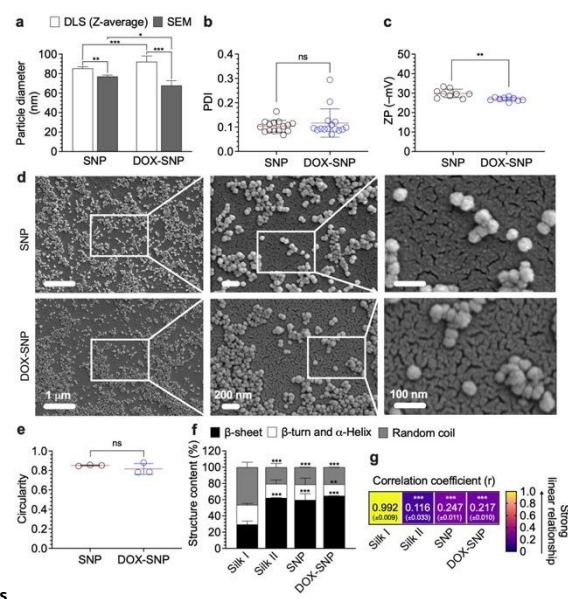


Fig. 1 Physicochemical properties of doxorubicin-loaded silk nanoparticles (DOX-SNPs; 100 μ M DOX): (a) Particle diameter; (b) PDI; (c) Zeta potential (ZP); (d) FE-SEM micrographs; (e) Circularity; (f) Secondary structure content; (g) Correlation coefficient (FTIR), determining the linear relationship of IR adsorption spectra using silk I structure as reference. $p < 0.1$ (*), $p < 0.01$ (**), $p < 0.001$ (***), $n = 3$.

This partial constraint is chemically significant, as β -sheet-rich domains regulate particle stability, chain mobility, and diffusion pathways, as β -sheet domains regulate silk chain mobility and diffusion pathways that govern drug retention and release. Formulation integrity and population heterogeneity were assessed using FI-AF4 coupled with MALS, DLS, and

^aStrathclyde Institute of Pharmacy and Biomedical Sciences, University of Strathclyde, 161 Cathedral St., Glasgow G4 0RE, Scotland, UK

^bFraunhofer Institute for Molecular Biology and Applied Ecology, Branch Bioresources, Ohlebergsweg 12, 35392 Giessen, Germany

^cFriedrich Schiller University Jena, Institute of Pharmacy, Department of Pharmaceutics and Biopharmaceutics, Lessingstr. 8, 07743 Jena, Germany

Corresponding author: Zahra Rattray, email: zahra.rattray@strath.ac.uk



spectroscopic detection (Fig. S6). Doxorubicin loading slightly alters nanoparticle size, shape factor, or aggregation behaviour; however, confirming that adsorption effectively preserves nanoparticle morphology (Fig. 2a, b, and Table S1).^{19, 20}

Single particle automated Raman trapping analysis provided direct evidence of formulation homogeneity. Characteristic doxorubicin Raman signatures were detected in ~95% of individual particles, with strong correlation across multiple diagnostic vibrational bands (Fig. 2c and Table S2–S3). Raman spectra of silk nanoparticles (421 to 1800 cm^{-1}) were dominated by protein features, including amide stretches, and phenylalanine, whereas, doxorubicin features slightly shifted relative to reported values (Fig. 2c and Table S2).^{21, 22} These changes likely reflect differences in excitation conditions and the local chemical environment.²¹ Despite partial overlap between doxorubicin and protein bands, doxorubicin-loaded nanoparticles showed a clear and consistent increase in drug-associated Raman signals across multiple diagnostic peaks (Fig. 2c).

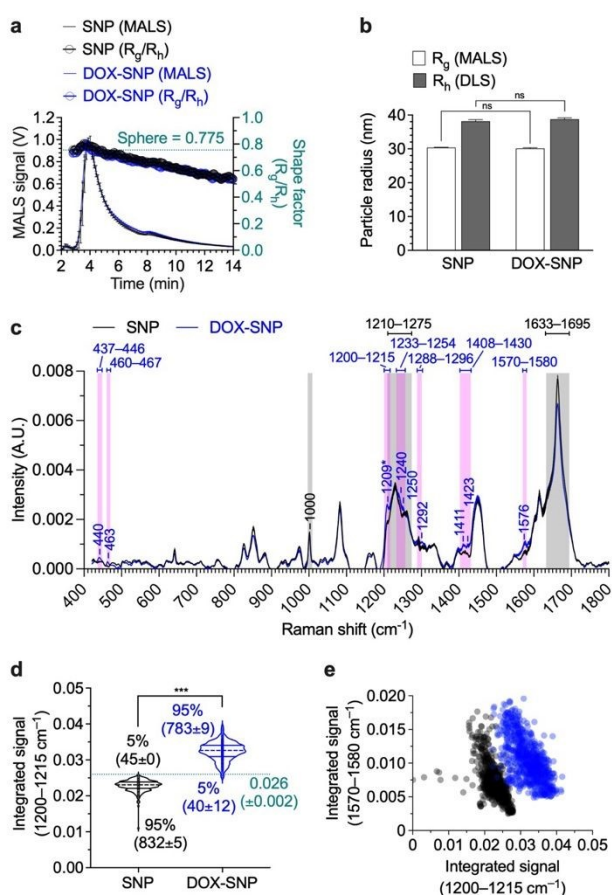


Fig. 2 FI-AF4 fractogram and SPARTA. (a) FI-AF4-MALS aligned with computed shape factor (R_y/R_h). Dotted line indicates ideal spherical shape factor of 0.775. (b) R_y and R_h were obtained from MALS and DLS detector measurements. (c) Overlay of Raman spectra (421–1800 cm^{-1}) for protein (black) and doxorubicin (pink). (d) Integrated Raman signal analysed by the univariate analysis mode. (e) Bivariate analysis, showing a signal intensity correlation of 1200–1215 and 1570–1580 cm^{-1} . $p < 0.1$ (*), $p < 0.01$ (**), $p < 0.001$ (***), $n = 3$.

Univariate and bivariate analyses confirmed a distinct separation between empty and drug-loaded particle populations, with particularly strong discrimination at 1209

cm^{-1} (Fig. 2d, e), indicating highly homogeneous drug incorporation (Fig. 2d, e, Fig. S7, and Fig. S8). A concomitant reduction in Raman intensity at 1660, 850, and 825 cm^{-1} corresponding to the Amide I (C=O) stretch at 1660 cm^{-1} and tyrosine residues at 850 and 825 cm^{-1} ,²³ suggests localised perturbation of the silk fibroin structure. These changes are consistent with hydrogen bonding between protonated doxorubicin and silk carbonyl groups, together with hydrophobic interactions involving tyrosine residues, supporting the formation of a surface-associated silk-doxorubicin complex (Fig. 2c). This single-particle insight confirms uniform drug distribution, overcoming a key limitation of ensemble-averaged measurements that obscure population heterogeneity. Subtle attenuation of specific protein Raman bands suggests local perturbation of the silk microenvironment upon drug binding, consistent with protein-drug complex formation at the particle surface.²⁴

Adsorption-loaded silk nanoparticles exhibited pronounced pH-dependent doxorubicin release under physiologically relevant conditions. Drug release increased systematically with decreasing pH, following the trend $\text{pH } 7.0 < 6.5 < 4.5$, reflecting protonation-driven weakening of electrostatic interactions and increased silk chain mobility below the isoelectric point of silk fibroin (Fig. 3a).^{10, 25} We speculated that both the physical stability of doxorubicin-loaded silk nanoparticle and dialysis is pH-dependent.²⁶ Therefore, doxorubicin encapsulation may further alter formulation stability under dialysis conditions, reducing the release rate and prolonging the release period.

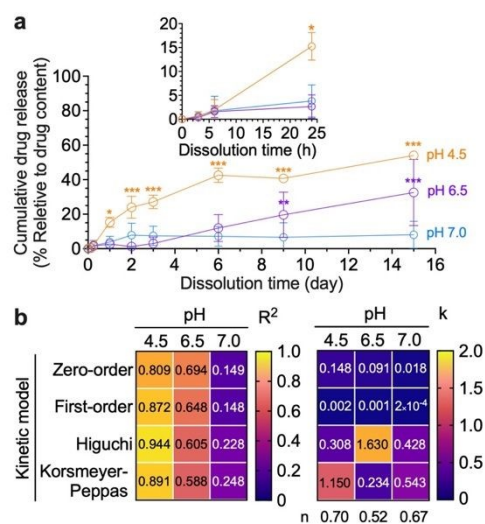


Fig. 3 *In vitro* drug release. Doxorubicin-loaded silk nanoparticles (DOX-SNPs; 100 μM DOX) were prepared at 1.5 mg protein, followed by dialysis against 2 mL of buffer (1 \times PBS pH 7.0, HEPES buffer pH 6.5, and citrate phosphate buffer pH 4.5) for 15 days; (a) Cumulative drug release; (b) Release kinetics. $p < 0.1$ (*), $p < 0.01$ (**), $p < 0.001$ (***), $n = 3$.



COMMUNICATION

Release kinetics were best described by diffusion-dominated models incorporating polymer relaxation (Higuchi and Korsmeyer-Peppas models), indicating diffusion-controlled release coupled with polymer relaxation (Fig. 3b and Fig. S9).^{27, 28}

As proof-of-concept evaluation of biological performance, silk nanoparticles were evaluated in MDA-MB-231 triple-negative breast cancer cells. Placebo nanoparticles exhibited negligible cytotoxicity, confirming biocompatibility. In contrast, doxorubicin-loaded nanoparticles demonstrated dose-dependent cytotoxicity comparable to free doxorubicin (Fig. 4a). Confocal imaging revealed time- and concentration-dependent uptake, with intracellular doxorubicin localising in perinuclear regions, consistent with its known mechanism of action. These results confirm that adsorption-mediated loading preserves pharmacological efficacy while enabling pH-responsive delivery (Fig. 4b-d).

The pH of the cell culture medium was maintained at approximately 7.4 by bicarbonate buffering. Based on the release profile at pH 7.0, only limited doxorubicin release from doxorubicin-loaded silk nanoparticles (~10%) was expected within 48 h of incubation. Together with the proposed cellular uptake mechanism, we hypothesized that doxorubicin-loaded silk nanoparticles were internalized *via* endocytosis and subsequently sequestered to lysosomes. Under these conditions, the acidic lysosomal environment (pH ~4.5) may enhance doxorubicin release, potentially increasing cumulative release to ~15% within 48 h (Fig. 3a). Nevertheless, *in vivo* DOX release should be further investigated, as current *in vitro* release methods may not fully reflect the release behaviour of doxorubicin-loaded silk nanoparticles under physiological conditions.

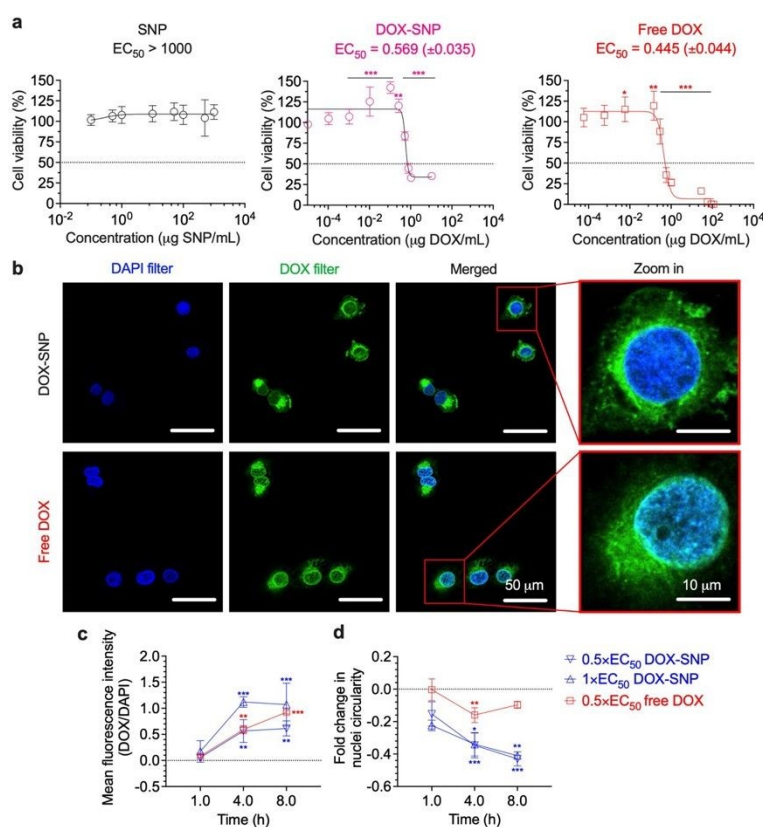


Fig. 4 Cellular responses in MDA-MB-231 cells. Cells were incubated with doxorubicin-loaded silk nanoparticles (DOX-SNPs; 100 μM DOX) for 48 h, followed by the CellTiter-Glo assay; (a) Dose-dependent cytotoxicity of placebo SNPs, DOX-SNPs, and doxorubicin; (b) Confocal images (63x) after 1 h exposure (0.5xEC₅₀); (c) DOX/DAPI intensity; (d) Fold-change in nuclear circularity after 1–8 h exposure. $p < 0.1$ (*), $p < 0.01$ (**), $p < 0.001$ (***), $n = 3$.



COMMUNICATION

In summary, this study established adsorption as a chemically tractable strategy for loading doxorubicin onto silk nanoparticles, coupling protein electrostatics and β -sheet structure to pH-responsive release while demonstrating high biocompatibility, retention of therapeutic efficacy, and potential selectivity toward cancer cells. Together, these findings support the rational design of tunable silk-based nanocarrier systems for targeted doxorubicin delivery.

Conflicts of interest

There are no conflicts to declare.

Author Contributions

NR wrote the manuscript, designed and conducted the experiments, and analysed the data. HG assisted with the use of the confocal microscope. PB assisted with the use of FI-AF4. FPS conceptualized and designed the study and edited the manuscript. ZR conceptualised and designed the study, analysed data, edited the manuscript, and acquired funding.

Acknowledgments

We thank Catherine Saunders for providing access to the SPARTA system. NR acknowledges funding from the Office of Educational Affairs, UK; the Royal Thai Embassy, Thailand; and the Office of the Civil Service Commission, Thailand, which provided a PhD scholarship. The authors acknowledge that the scanning electron microscopy work was carried out at the Advanced Materials Research Laboratory at the University of Strathclyde. ZR and FPS thank the Engineering and Physical Sciences Research Council (EP/V028960/1) for financial support.

Data availability

All data associated with this work are included in the supplementary information or can be accessed at <https://doi.org/10.15129/ed1bb0a8-6eff-434f-8355-ac5ede92b5b9>.

Abbreviations

B. mori, *Bombyx mori*; DAPI, 4',6-diamidino-2-phenylindole; DLS, Dynamic Light Scattering; DOX, Doxorubicin; DOX-SNP, Doxorubicin-

loaded silk nanoparticle; EC₅₀, half-maximal effective concentration; ELS, Electrophoretic Light Scattering; FE-SEM, Field-Emission Scanning Electron Microscopy; FI-AF4, Frit-Inlet Asymmetric Flow Field-Flow Fractionation; FTIR, Fourier-Transform Infrared; IPA, Isopropanol; LiBr, Lithium bromide; MALS, Multiangle Light Scattering; Na₂CO₃, Sodium carbonate; PDI, Polydispersity index; R_g, Radius of gyration; R_h, Hydrodynamic radius; SNP, Silk nanoparticle; SPARTA, Single Particle Automated Trapping Analysis; UV, Ultra-Violet; X-Flow, Cross-Flow; ZP, Zeta potential

References

1. A. Bisht, D. Avinash, K. K. Sahu, P. Patel, G. Das Gupta and B. D. Kurmi, Drug Delivery and Translational Research, 2025, 15, 102-133.
2. S. A. L. Matthew and F. P. Seib, Advanced Therapeutics, 2025, 8, 2400130.
3. I. C. Jones and C. R. Dass, Journal of Pharmacy and Pharmacology, 2022, 74, 1677-1688.
4. U. Bulbake, S. Doppalapudi, N. Kommineni and W. Khan, Pharmaceutics, 2017, 9, 12.
5. A. Fukuda, K. Tahara, Y. Hane, T. Matsui, S. Sasaoka, H. Hatahira, Y. Motooka, S. Hasegawa, M. Naganuma and J. Abe, PLoS One, 2017, 12, e0185654.
6. M. A. Asensio Ruiz, Á. Alonso García, M. d. I. L. Bravo-Ferrer Moreno, I. Cebreiros-López, J. A. Noguera-Velasco, A. A. Lozano-Pérez and T. Martínez Martínez, Pharmaceutics, 2023, 16, 248.
7. S. Gou, Y. Huang, Y. Wan, Y. Ma, X. Zhou, X. Tong, J. Huang, Y. Kang, G. Pan and F. Dai, Biomaterials, 2019, 212, 39-54.
8. F. P. Seib, AIMS bioengineering, 2017, 4, 239-258.
9. J. Kundu, Y.-I. Chung, Y. H. Kim, G. Tae and S. C. Kundu, International journal of pharmaceutics, 2010, 388, 242-250.
10. F. P. Seib, G. T. Jones, J. Rnjak-Kovacina, Y. Lin and D. L. Kaplan, Advanced healthcare materials, 2013, 2, 1606-1611.
11. J. D. Totten, T. Wongpinyochit and F. P. Seib, Journal of drug targeting, 2017, 25, 865-872.
12. S. Shaidani, C. Jacobus, J. K. Sahoo, K. Harrington, H. Johnson, O. Foster, S. Cui, O. Hasturk, T. Falcucci and Y. Chen, ACS Applied Nano Materials, 2023, 6, 18967-18977.
13. B. Yu, Y. Li, Y. Lin, Y. Zhu, T. Hao, Y. Wu, Z. Sun, X. Yang and H. Xu, Frontiers in Pharmacology, 2023, 13, 1071868.
14. S. Bhattacharjee and D. J. Brayden, Expert opinion on drug discovery, 2021, 16, 235-254.
15. A. Bhadran, H. Polara, G. K. Babanyinah, S. Baburaj and M. C. Stefan, Cancers, 2025, 17, 2303.
16. T. N. Saeed, A. F. Al-Hussainy, G. Sanghvi, S. Ballal, A. Singh, T. Sudhakar, S. Mishra, A. Kubaev, S. G. Taher and M. Alwan, Journal of Drug Delivery Science and Technology, 2025, 107649.



17. W. Cai, M. Guo, X. Weng, W. Zhang and Z. Chen, *Materials Science and Engineering: C*, 2019, 98, 65-73.
18. C. Racles, M.-F. Zaltariov, D. Peptanariu, T. Vasiliu and M. Cazacu, *Nanomaterials*, 2022, 12, 1823.
19. M. Wang, W. Zhang, L. Yang, Y. Li, H. Zheng and H. Dou, *Food Chemistry: X*, 2024, 22, 101267.
20. A. M. Striegel, *Macromolecular separation science*, Springer Nature, 2025.
21. P. V. A. Pessanha and A. C. Sant'Ana, *Journal of the Brazilian Chemical Society*, 2025, 36, e-20250121.
22. R. Zhang, J. Zhu, D. Sun, J. Li, L. Yao, S. Meng, Y. Li, Y. Dang and K. Wang, *Micromachines*, 2022, 13, 940.
23. J. Guo, W. Cai, B. Du, M. Qian and Z. Sun, *Biophysical chemistry*, 2009, 140, 57-61.
24. J. Penders, I. J. Pence, C. C. Horgan, M. S. Bergholt, C. S. Wood, A. Najer, U. Kauscher, A. Nagelkerke and M. M. Stevens, *Nature communications*, 2018, 9, 4256.
25. C. W. P. Foo, E. Bini, J. Hensman, D. P. Knight, R. V. Lewis and D. L. Kaplan, *Applied Physics A*, 2006, 82, 223-233.
26. N. Roamcharern, P. Punnabhum, F. P. Seib and Z. Rattray, *Nanoscale advances*, 2025, 7, 5519-5535.
27. A. Szepes, Z. Makai, C. Blümer, K. Mäder, P. Kása Jr and P. Szabó-Révész, *Carbohydrate polymers*, 2008, 72, 571-578.
28. P. I. P. Soares, A. I. Sousa, J. C. Silva, I. M. M. Ferreira, C. M. M. Novo and J. P. Borges, *Carbohydrate polymers*, 2016, 147, 304-312.

View Article Online
DOI: 10.1039/D6CC02515C



View Article Online
DOI: 10.1039/D6CC02515C

All data associated with this work are included in the supplementary information or can be accessed at <https://doi.org/10.15129/ed1bb0a8-6eff-434f-8355-ac5ede92b5b9>.

